Nanoparticles and microfluidics for future tuberculosis vaccines

Neustrup, M.A.

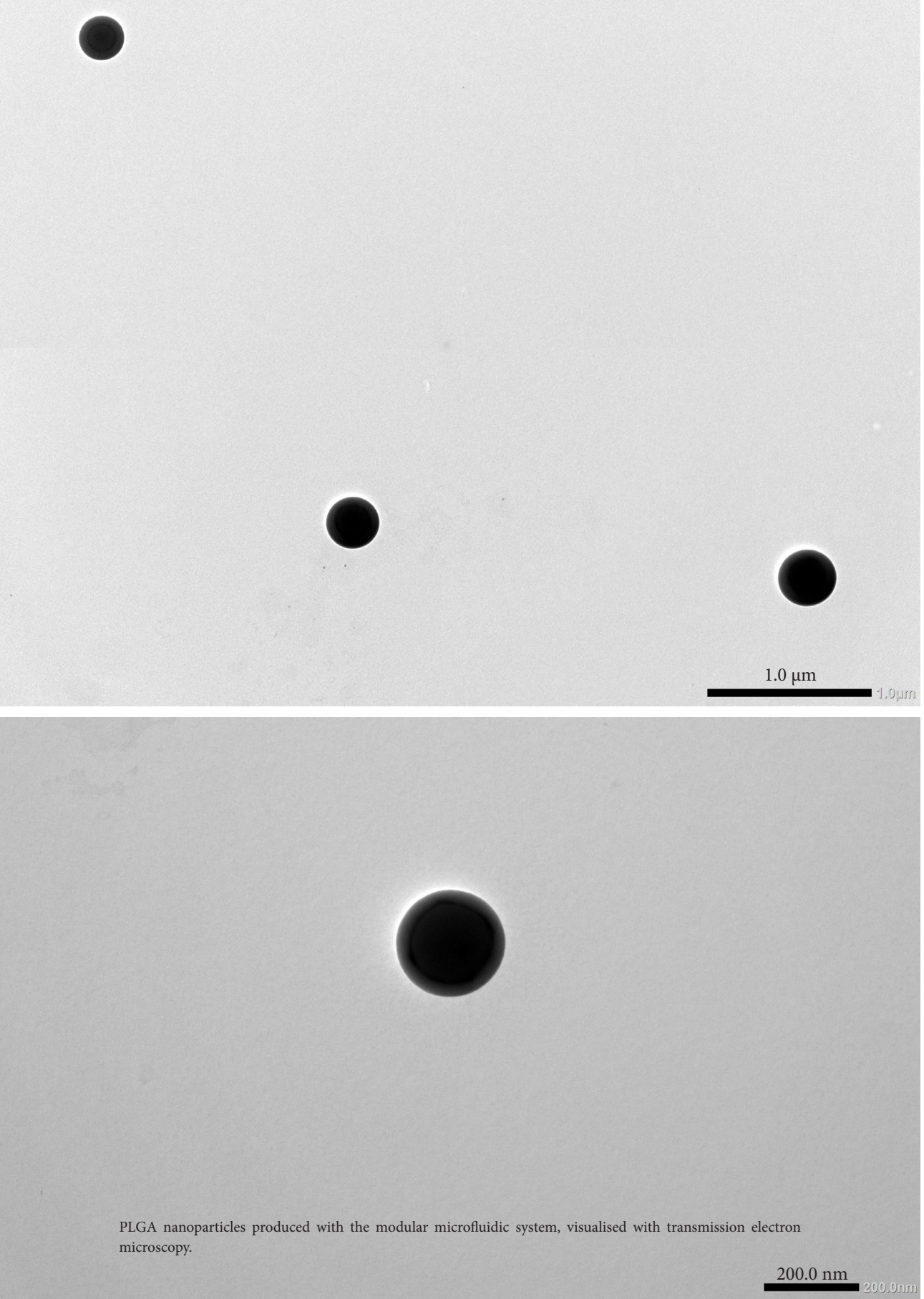

PLGA nanoparticles produced with the modular microfluidic system, visualised with transmission electron microscopy.

CHAPTER 3

A VERSATILE, LOW-COST MODULAR MICROFLUIDIC SYSTEM TO PREPARE POLY(LACTIC-*CO*-GLYCOLIC ACID) NANOPARTICLES WITH ENCAPSULATED PROTEIN

Adapted from Pharm Res. 2024;41(12):2347-61

M.A. Neustrup[1,2], T.H.M. Ottenhoff[2], W. Jiskoot[1], J.A. Bouwstra[1], K. van der Maaden[1,3]

[1] Division of BioTherapeutics, Leiden Academic Centre for Drug Research, Leiden University, Leiden, The Netherlands
[2] Department of Infectious Diseases, Leiden University Medical Center, Leiden, The Netherlands
[3] Tumor Immunology Group, Department of Immunology, Leiden University Medical Center, Leiden, The Netherlands

ABSTRACT

Microfluidics has emerged as a promising technique to prepare nanoparticles. However, the current microfluidic devices are mainly chip-based and are often integrated into expensive systems that lack on-the-spot versatility. The aim of this study was to set up a modular microfluidic system based on low-cost capillaries and reusable, easy-to-clean building blocks that can prepare poly(D,L-lactic-*co*-glycolic acid) (PLGA) nanoparticles with and without incorporated water-soluble biomacromolecules. A two-syringe system variant of the microfluidic system was set up to prepare PLGA particles and to investigate how the flow rates, solvents, and PLGA concentrations impacted the PLGA nanoparticle formation. A three-syringe system was designed to examine the incorporation of proteins into the PLGA particles. The formation of the nanoparticles was affected by the PLGA concentration in the organic solvent, where an increasing concentration led to larger particle diameters (33–180 nm), and by the total flow rate, where an increase in the total flow rate led to smaller nanoparticles (197–77 nm). Using ultrapure water as the aqueous solvent resulted in precipitation at the outlet at higher PLGA concentrations. Aqueous poly(vinyl alcohol) created neutral particles in contrast to the negatively charged particles obtained with ultrapure water or an ethanol-water mixture. Incorporation of the proteins ovalbumin or lysozyme with a three-syringe system resulted in encapsulation efficiencies above 40%. A cheap and easily adjustable modular microfluidic system was developed to prepare PLGA nanoparticles with highly reproducible particle diameters that can effectively be loaded with proteins for drug and vaccine delivery.

INTRODUCTION

Poly(D,L-lactic-*co*-glycolic acid) (PLGA) nanoparticles fall in the size range of 10–1,000 nm [1] an are suitable for a wide range of biomedical applications, as reviewed elsewhere [2]. They have an excellent safety profile, being both biodegradable and biocompatible [3], and their properties are adjustable, allowing for the customisation of their properties to fit specific applications. For instance, the degradation rate of the particles, and thereby the release of the encapsulated drug or contrast agent, is tunable, as particles made with a PLGA polymer with higher hydrophilicity, lower crystallinity, or lower molecular weight tend to degrade faster [3]. PLGA nanoparticles are widely used in preclinical studies where they, among others, have been used in imaging [4], cancer therapies [5], as well as (subunit) vaccines with peptides [6] and proteins [7]. PLGA polymer is already approved as an excipient for human parenteral use by the U.S. Food and Drug Administration, mainly as a microparticle component of depot formulations in antibiotics, antipsychotics, diabetes, plus medications against cancer and hormonal diseases [8]. As PLGA-based products are already approved, it signifies a promising future for PLGA nanoparticles, making them an attractive option for the development of next-generation drug delivery systems with their great tunability and safety.

PLGA nanoparticles are mainly produced by two methods: emulsion-based methods, where a water-immiscible or partly water-immiscible organic solvent containing dissolved PLGA is emulsified in an aqueous solution with a surfactant, and nanoprecipitation methods, where a water-miscible organic solvent containing dissolved PLGA is mixed with an aqueous solution [9, 10]. The emulsification process is conventionally carried out with techniques such as sonication, high-shear mixing, or high-pressure homogenisation, while nanoprecipitation usually is carried out by adding an organic solvent with dissolved PLGA drop-wise to an aqueous formulation under mechanical stirring [9, 10]. While these techniques allow for manipulation of the nanoparticle diameter by varying factors, such as the PLGA concentration and the surfactant concentration [10], the batch-to-batch reproducibility is low [11], and the nanoparticles are rarely below 100 nm [10]. Microfluidics, a technique that enables the manipulation of fluid streams through microscale fluidic channels, has emerged to overcome these problems, offering precise control of the nanoparticle diameter, greater batch-to-batch reproducibility, and a narrower particle size distribution [12]. While emulsion-based microfluidics, also called droplet-based microfluidics, tend to generate micrometre-sized particles, nanoprecipitation microfluidics, also called continuous microfluidics, tend to generate nano-sized particles [13]. This particle diameter control is particularly important in vaccination, where the particle diameter and other factors, such as surface charge and rigidity, affect the cellular uptake and influence the immune response [14–16]. In addition to size control, microfluidics can reduce solvent waste during production and result in shorter preparation times, as it allows for one-step nanoparticle assembly [10].

Incorporation of active pharmaceutical ingredients into PLGA micro- and nanoparticles using microfluidic systems has mainly been applied for small hydrophobic drugs, such as bupivacaine, risperidone, ibuprofen, and paclitaxel, and small hydrophilic drugs such as doxorubicin hydrochloride [13]. Only very few research groups study the incorporation of large water-soluble biomacromolecules, such as proteins, with microfluidic systems. Recently, the proteins ovalbumin, bovine serum albumin, and a fusion protein have been incorporated into PLGA nanoparticles (with different lactide-to-glycolide ratios) with encapsulation efficiencies ranging from 7 to 38% with loading capacities of 0.5 to 3.1 wt% with a microfluidic system [17]. That study used a microfluidic system called Nanoassemblr®, which combines two fluids via a herringbone [17]. Although the Nanoassemblr® system can incorporate various compounds into PLGA nanoparticles, the system is quite expensive and cannot easily be rebuilt for formulations requiring more optimisation.

In this research, we developed a versatile, low-cost modular microfluidic system that enables the combination of multiple fluid flows. As a starting point, a two-syringe system, whose fluids meet in a co-flow, was set up to determine critical parameters for the preparation of the PLGA nanoparticles. Different solvents, PLGA concentrations, and solvent flows were used to delimit how these factors affect nanoparticle formation. Based on these results, a three-syringe system was designed to incorporate two water-soluble proteins with different physicochemical properties: i) ovalbumin, a protein with a molecular size of 42.7 kDa [18] which is negatively charged at pH 7.4 [19], and ii) lysozyme, a protein with a molecular size of 14.3 kDa [20], which is positively charged at pH 7.4 [21]. Using our novel nanoparticle preparation system, we obtained PLGA nanoparticles with tunable nanoparticle diameters and well-defined physicochemical properties. Moreover, we show that proteins with different properties are effectively loaded into PLGA nanoparticles using this modular microfluidics system.

MATERIALS AND METHODS

Materials

NE300 syringe pumps were purchased from ProSense B.V. (Oosterhout, The Netherlands). Pierce Micro bicinchoninic acid protein assay kit, 500 µL Hamilton® Gastight® syringes from the 1700 series with polytetrafluoroethylene (PTFE) Luer-lock terminations, disposable polystyrene BRAND® Macro cuvettes, and polyether ether ketone (PEEK) capillary tubing with an inner diameter (ID) of 0.02" (0.5 mm) and an outer diameter (OD) of 1/16" (1.6 mm), were bought from Fisher Emergo B.V. (Landsmeer, the Netherlands). 10 mL Hamilton® Gastight® syringes from the 1000 series with PTFE Luer-lock termination were purchased from Brunschwig Chemie B.V (Amsterdam, the Netherlands). A PTFE tube with an ID of 1.6 mm was purchased from Waters Chromatography B.V. (Etten-Leur, the Netherlands). The following CapTite™ microfluidic components were purchased from Mengel Engineering (Virum, Denmark): one-piece fittings in PEEK for tubes with an ID of 1/16" (1.6-mm fittings), one-piece fittings in PEEK for capillaries with an ID of 360 µm (360-µm fittings), female fitting Luer-lock adapters in PEEK for capillaries with an ID of 360 µm (Luer-lock adapters), 360 µm to 1/16" two-piece adapters in PEEK (360-µm-to-1.6-mm adapters), 1/16" to 360 µm two-piece adapters in PEEK (1.6-mm-to-360-µm adapters), interconnect tee in Ultem® 1000 resin (untreated polyetherimide) for tubes with an ID of 1/16" (1.6-mm-interconnect tee) and interconnect tee in Ultem® 1000 polyetherimide for capillaries with an ID of 360 µm (360-µm-interconnect tee). Polyimide-coated fused silica capillary tubing with IDs of 75 ± 3 µm and 250 ± 6 µm with IDs of 363 ± 10 µm and 360 ± 10 µm, respectively, were purchased from BGB Analytic Benelux B.V. (Harderwijk, the Netherlands). Poly(D,L-lactic-*co*-glycolic acid) (PLGA) (acid terminated, lactide:glycolide 50:50, Mw 24,000-38,000), sodium dodecyl sulphate with a minimum purity of 99.0%, sodium phosphate dibasic dihydrate with a purity of 99.5%, sodium phosphate monobasic dihydrate with a minimum purity of 99.0%, and pure sodium hydroxide pellets were purchased from Merck Chemicals B.V. (Amsterdam, the Netherlands). Lysozyme from chicken egg white with a protein content not less than 90% (measured with UV absorbance) (pI 11.35, electrophoretic analyses were performed in buffers of ionic strength of 0.1 [21]) and poly(vinyl alcohol) (Mw ~31,000) (PVA) were purchased from Sigma-Aldrich Chemie B.V. (Zwijndrecht, the Netherlands). Analytical grade dimethyl sulfoxide (DMSO) with a purity over 99% and HPLC-R grade acetonitrile with a purity over 99.9% were purchased from Biossolve B.V. (Valkenswaard, the Netherlands). EndoFit™ Ovalbumin (chicken egg albumin for in-vivo use) (pI 4.4, measured in 10 mM phosphate buffer at a concentration of 1 mg/mL [19]) with a minimum purity of 98% was purchased from InvivoGen®, Bio-Connect B.V. (Huissen, the Netherlands). Ethyl acetate with a minimum purity of 99.9 vol%, 96 vol% ethanol, and acetone with a minimum purity of 99.8 vol% were purchased from Boom B.V. (Meppel, the Netherlands). Spectra-Por® Milli-Q® water (ultrapure water), with a resistivity of 18.2 MΩ/cm at 25°C, was tapped from a Milli-Q® Advantage A10 water purification system (Merck).

Setup of the microfluidic system

The PLGA nanoparticles were prepared with a modular microfluidic system assembled as either a two-syringe system or a three-syringe system, as depicted in Fig. 1. To assemble the core component, a 1.6-mm-interconnect tee with three ports in a T shape designated Port 1, Port 2, and Port 3, where Port 1 and 3 were opposite of each other, and Port 2 was positioned at an angle of 90°, was connected through Port 3 to a 7 cm long piece of PEEK tube with a 1.6-mm fitting. A 360-µm-to-1.6-mm adapter was attached to a Luer-lock adapter and screwed on Syringe 1 (a 10-mL syringe). Hereafter, a 20 cm long PTFE tube with an ID of 1.6 mm was attached to it with a 1.6-mm fitting. The other end of the PTFE tube was connected to Port 2 with a 1.6-mm fitting. When the tubes were attached, they were first pushed fully into the 1.6-mm-interconnect tee before the 1.6-mm fitting was screwed on. A 1.6-mm-to-360-µm adapter was connected to Port 1.

As the first step of assembling the attachment of the two-syringe system, a Luer-lock adapter was screwed on Syringe 2 (a 10-mL syringe). A 14 cm long capillary with an ID of 250 µm was attached to the Luer-lock adapter with a 360-µm fitting. When the capillary was attached to the Luer-lock adapter, the capillary was pushed to the end of the 360-µm fitting tip before insertion. The other end of the capillary was attached to the core component by inserting it through a 360-µm fitting and pushing it through the 1.6-mm-interconnect tee and PEEK tube till it reached 1 cm through the PEEK tube, after which the 360-µm fitting was screwed on the 1.6-mm-to-360-µm adapter.

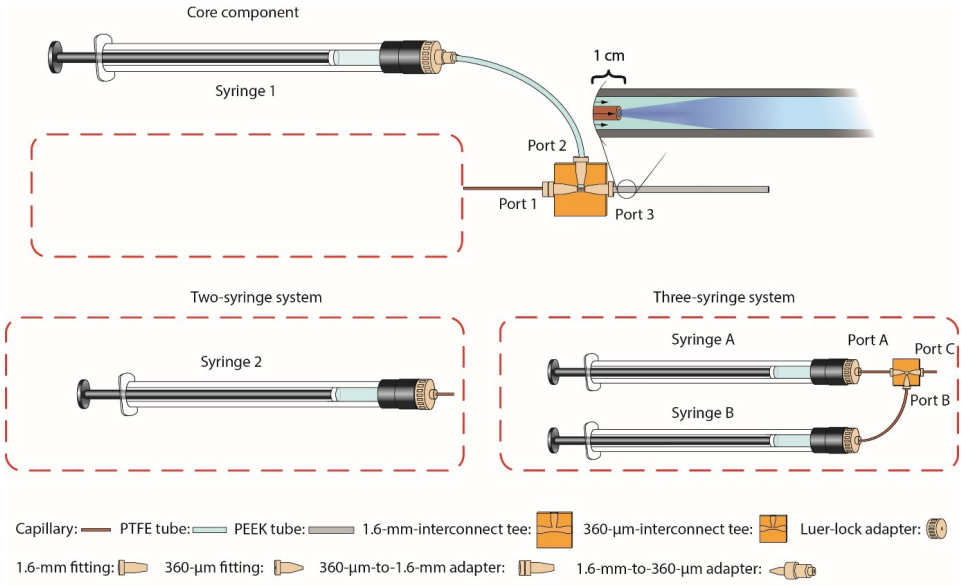

Figure 1. Schematic representation of the modular microfluidic system. The core component consists of Syringe 1 that is connected through a clear tube to an interconnect tee (yellow). A capillary (brown) passes laterally through the interconnect tee (via Ports 1 and 3) and extends 1 cm into the PEEK tube (grey). This allows for a co-flow, where the fluid from Syringe 1 constitutes the outer flow. The fluid from the capillary constitutes the inner flow and comes either from Syringe 2, making it a two-syringe system, or the combined fluid from Syringe A and Syringe B, making it a three-syringe system. PTFE: polytetrafluoroethylene, PEEK: polyether ether ketone.

As the first step of assembling the attachment for the three-syringe system, Luer-lock adapters were screwed on Syringe A (a 500-µL syringe) and Syringe B (a 10-mL syringe). Two 14 cm long capillaries with IDs of 75 µm and 250 µm were attached to the Luer-lock adapters with 360-µm fittings on Syringe A and Syringe B, respectively. A 360-µm-interconnect tee with three ports in a T shape designated Port A, Port B, and Port C, where Port A and C were opposite of each other, and Port B was positioned at an angle of 90° from Port A and B, was connected through Port A to the capillary from Syringe A with a 360-µm fitting. The capillary from Syringe B was connected to Port B with a 360-µm fitting. Port C was connected to a 14 cm long capillary with an ID of 250 µm using a 360-µm fitting. The other end of the capillary attached to Port C was attached to the core component, as explained in the setup of the two-syringe system.

To complete the setup, the syringes were mounted on syringe pumps. When the formulations were collected from the end of the PEEK tube, the tube was held perpendicular to the sample collectors, and an initial volume of approximately 150 µL was discarded before the sample was tapped.

Preparation of PLGA nanoparticles

Effect of solvent and PLGA concentration on nanoparticle formation

The solvents and the concentration of PLGA used in the microfluidic system may play a role in the formation and properties of the formed PLGA nanoparticles. A two-syringe system was employed to investigate how six different solvents and nine PLGA concentrations influence the formation and characteristics of the resulting nanoparticles. The total flow rate (TFR) and the flow rate ratio (FRR) were held constant at values of 5.00 mL/min and 1:3 between Syringe 2 and 1, respectively. The organic solvent in Syringe 2, where PLGA was dissolved, was acetone or acetonitrile. The aqueous solvent in Syringe 1 was ultrapure water, 20 mg/mL PVA filtered through a 0.22 µm filter, or 96 vol% ethanol mixed 1:1 (v/v) with ultrapure water (ethanol-water mixture). In total, six solvent combinations were tested: 1) acetone and ultrapure water, 2) acetone and ethanol-water mixture, 3) acetone and 20 mg/mL PVA, 4) acetonitrile and ultrapure water, 5) acetonitrile and ethanol-water mixture, and 6) acetonitrile and 20 mg/mL PVA. For each solvent combination, nine concentrations of PLGA in the organic phase were tested (0.25, 0.5, 1, 3, 5, 7, 10, 15, and 20 mg/mL). All samples were prepared in triplicate on different days, and each sample was measured three times.

Effect of flow rate on nanoparticle formation

The flow rates of the organic and aqueous fluids in the modular microfluidic system may affect the formation and properties of the formed PLGA nanoparticles. The effect of five different FRRs and eight TFRs variations on the particle formation and characteristics was investigated with the two-syringe system. A PLGA concentration of 3 mg/mL in acetonitrile was selected in combination with an ethanol-water mixture as the aqueous phase (as optimised in section 2.3.1.). To test the effect of the FRR, the TFR was held constant at 5.00 mL/min and the FRRs between the fluid in Syringe 2 and Syringe 1 were set to either 1:1, 1:2, 1:3, 1:4, or 1:5. To test the effect of the TFR, the FRR between the fluid in Syringe 1 and Syringe 2 was held constant at 1:3, and the TFRs were set to either 0.100, 0.500, 1.00, 2.00, 3.00, 4.00, 5.00, or 6.00 mL/min. All samples were prepared in triplicate on different days, and each sample was measured in triplicate. The various variables are summarised in Table 1.

Table 1. Different variables were examined in this work with the two-syringe system.

Examined	Variables	Constants
Section 2.3.1.	**Solvent in Syringe 1**	**FRR**
	Ultrapure water	1:3 between Syringe 2 and 1
	20 mg/mL PVA in ultrapure water	
PLGA concentrations and solvents	Ethanol-water mixture	
	Solvent in Syringe 2	**TFR**
	Acetone	5,000 µL/min
	Acetonitrile	
	PLGA concentration	
	0.25, 0.5, 1, 3, 5, 7, 10, 15, or 20 mg/mL	
Section 2.3.2.	**FRR between Syringe 2 and 1**	**Solvent in syringe 1**
	1:1, 1:2, 1:3, 1:4, or 1:5	10 mg/mL PVA in ultrapure water
		Solvent in Syringe 2
FRR		Acetonitrile
		PLGA concentration
		3 mg/mL
		TFR
		5,000 µL/min
Section 2.3.2.	**TFR**	**Solvent in syringe 1**
	0.100, 0.500, 1.00, 2.00, 3.00, 4.00, 5.00, or 6.00 mL/min	10 mg/mL PVA in ultrapure water
		Solvent in Syringe 2
TFR		Acetonitrile
		PLGA concentration
		3 mg/mL
		FRR
		1:3 between Syringe 2 and 1

FRR: flow rate ratio, TFR: total flow rate, PVA: poly(vinyl alcohol), PLGA: Poly(D,L-lactic-*co*-glycolic acid).

Encapsulation of proteins in PLGA nanoparticles

To study the incorporation of biomacromolecules in PLGA nanoparticles with the modular microfluidic system, two differently charged proteins were investigated in the three-syringe system (see Fig. 1) at different concentrations. Ovalbumin and lysozyme, the selected proteins, have a negative and a positive charge at physiological pH, respectively. The flow rates used for incorporating both proteins were 3.700, 0.050, and 1.250 mL/min for Syringes 1, A, and B, respectively, and the content of Syringe 1 was 10 mg/mL PVA. For incorporating ovalbumin into the PLGA nanoparticles, the content of Syringe B was 5 mg/mL PLGA in acetonitrile, and the content of Syringe A was ovalbumin in ultrapure water where seven ovalbumin concentrations were tested: 0, 1.25, 2.5, 5.0, 7.5, 10.0, 12.5 mg/mL.

For incorporating lysozyme into the PLGA nanoparticles, the content of Syringe B was 2 mg/mL PLGA in acetonitrile, and the content of Syringe A was lysozyme in ultrapure water where seven lysozyme concentrations were tested: 0, 0.5, 1.0, 2.0, 3.0, 4.0, 5.0 mg/mL. All samples were prepared in triplicate. After preparation, the organic solvents in the formulations were evaporated under a stream of nitrogen, and the nanoparticle diameters and zeta potentials were measured. For the encapsulation efficiency measurements, the obtained formulations were added to 2 mL Eppendorf vials and diluted with ultrapure water to obtain formulations with a PLGA concentration of 0.5 mg/mL.

Characterisation of the PLGA nanoparticles

Determination of the encapsulation efficiencies of ovalbumin and lysozyme

The encapsulation efficiencies of ovalbumin and lysozyme in the protein-loaded PLGA nanoparticles were determined. To determine the encapsulation efficiencies, samples were taken before centrifugation and from the supernatant after centrifugation in a Microfuge® 18 centrifuge (14,000 g, 30 min, Beckman Coulter Nederland B.V., Woerden, the Netherlands).

The samples were mixed in the volume ratio 1:1 with a mixture of 30 vol% DMSO, 0.1 M NaOH, and 10 mg/mL sodium dodecyl sulphate to disrupt the PLGA nanoparticles and incubated at 37 °C for 2 h. The standard curve was prepared with either ovalbumin or lysozyme in 15 vol% DMSO, 0.05 M NaOH, and 5 mg/mL sodium dodecyl sulphate. Each sample was prepared in triplicate and plated on a transparent flat-bottom 96-well plate (Greiner Bio-One B.V., Alphen aan den Rijn, The Netherlands). The amounts of ovalbumin or lysozyme were quantified with a micro bicinchoninic acid assay following the manufacturer's instructions. The absorbance was measured at 562 nm with a plate reader (Tecan Spark®, Männedorf, Switzerland) with the software SparkControl v3.1.
The encapsulation efficiency (EE%) was calculated using the following equation:

$$\mathrm{EE\%} = \frac{C(\textit{total protein}) - C(\textit{protein in the supernatant})}{C(\textit{total protein})} \cdot 100\%$$

Where *C(total protein)* is the concentration of either ovalbumin or lysozyme measured in the sample before it was spun down, and *C(protein in the supernatant)* is the concentration of either ovalbumin or lysozyme in the supernatant after the nanoparticles were spun down.

Determination of the particle's diameter and the zeta potential

The empty PLGA nanoparticles and the nanoparticles with proteins incorporated were measured on a Zetasizer Nano ZS equipped with a helium-neon laser (Malvern Panalytical B.V., Almelo, the Netherlands) with Zetasizer Software v7.13 to determine the intensity-weighted mean hydrodynamic particle diameters (particle diameters) and polydispersity indexes (PDIs) with dynamic light scattering (measured at a detection angle of 173°), and the zeta potentials with laser Doppler electrophoresis. Before the measurements, the

formulations were diluted in 10 mM phosphate buffer (7.5 mM Na_2HPO_4, 2.5 mM NaH_2PO_4, pH 7.4) and added to disposable BRAND™ Macro cuvettes. The zeta potential was measured with a universal dip cell (Malvern Panalytical B.V.). The measurements were performed in technical triplicates.

Statistical analyses

The data were analysed in GraphPad Prism® version 8.0.1 (GraphPad Software, CA, USA). The data were analysed with the correlation tool to investigate the relationship between the PLGA concentration, TFR, or FRR and the particle diameter, PDI, or zeta potential. Each batch was treated as an individual value, adding to the degrees of freedom. The Pearson correlation coefficient was used to determine if the correlation between the variables was positive, negative, or if there was no correlation. The significances of the correlation coefficients were determined with two-tailed tests where a p-value of < 0.05 was considered significant. A one-way analysis of variance, followed by Tukey's multiple comparisons test, was performed to compare the means where $p < 0.05$ was considered statistically significant. To determine if the solvents impacted the relationship between the PLGA concentrations and particle diameters, the significance of the difference between two slopes was calculated where $p < 0.05$ was considered statistically significant.

RESULTS

Increasing the PLGA concentration in the organic phase results in larger nanoparticles

Empty PLGA nanoparticles were prepared using the modular microfluidic system with different solvents and PLGA concentrations. Independent of the organic phase (acetone or acetonitrile) and aqueous phase (ultrapure water, 20 mg/mL PVA in ultrapure water, or an ethanol-water mixture), an increased PLGA concentration resulted in an increased particle diameter of the formed nanoparticles (see Fig. 2). The solvent choice and the PLGA concentration affected the zeta potential. At higher PLGA concentrations, the formed nanoparticles became more monodisperse (as indicated by a lower PDI).

When the aqueous phase consisted of ultrapure water, a PLGA deposit at the tip of the PEEK tube was observed at higher PLGA concentrations. The deposit was observed from 3 mg/mL when PLGA was dissolved in acetone and from 7 mg/mL when PLGA was dissolved in acetonitrile. No deposits were observed when the solvent in the aqueous phase was the ethanol-water mixture or 20 mg/mL PVA in ultrapure water. The largest particle diameter was generated in the system with 20 mg/mL PLGA in acetone as the organic phase and 20 mg/mL PVA in ultrapure water as the aqueous phase, where the particle diameter reached 181 nm, and the smallest with 0.5 mg/mL acetone as an organic phase with 20 mg/mL PVA in ultrapure water, where the particle diameter reached 33 nm. The PDIs were below 0.3 for all the formulations except those prepared with PLGA concentrations below 1 mg/mL PLGA and 20 mg/mL PVA in ultrapure water in the aqueous phase. The zeta potentials were below -16 mV when the formulations were prepared with ultrapure water or ethanol-water mixture in the aqueous phase (Fig. 3). When the formulations were prepared with 20 mg/mL PVA in ultrapure water in the aqueous phase, the nanoparticles were hardly not charged (zeta potentials between -5 to 0 mV).

Correlation statistics were performed to see if there were positive or negative correlations between the PLGA concentration and the particle diameters (see Table 2) (see Table S1 for the PDIs and zeta potentials). There were statistically significant positive correlations between the PLGA concentrations and particle diameter for all the solvent combinations (see Table 1 for the solvent combinations), meaning that increasing PLGA concentrations resulted in larger particles. Significant negative correlations existed between the PLGA concentration and the zeta potential for the solvent combinations without PVA, which instead had significant positive correlations, and the PLGA concentrations and the PDIs for all solvent combinations except for acetone and the ethanol-water mixture.

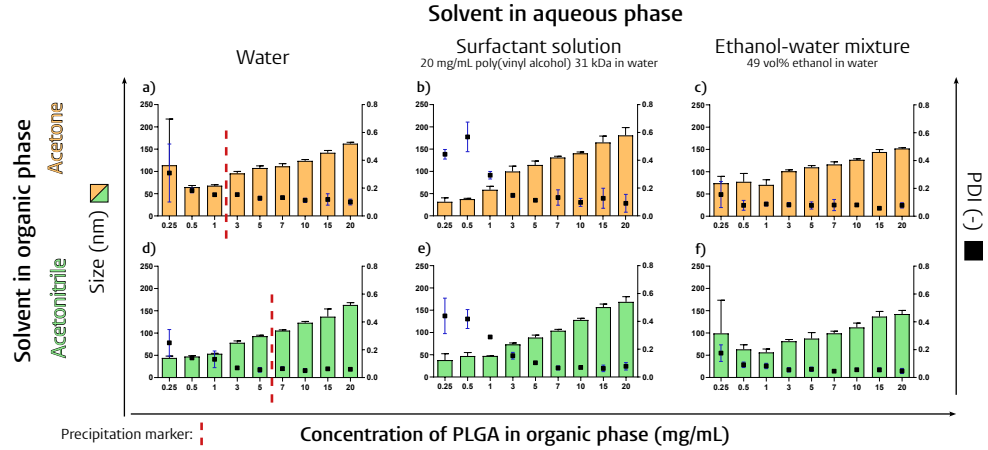

Figure 2. The influence of the PLGA concentration in the organic phase on the particle diameter and PDI of the formed PLGA nanoparticles, where the organic and aqueous phase consisted of a) acetone and ultrapure water, b) acetone and PVA in ultrapure water, c) acetone and an ethanol-water mixture d) acetonitrile and ultrapure water, e) acetonitrile and PVA in ultrapure water, f) and acetonitrile and an ethanol-water mixture, respectively. The TFR was 5,000 µL/min, and the FRR between the organic and the aqueous phase was 1:3. The precipitation marker indicates where the PLGA started to precipitate at the tip of the PEEK tube. Mean ± SD, n = 3. PDI: polydispersity index.

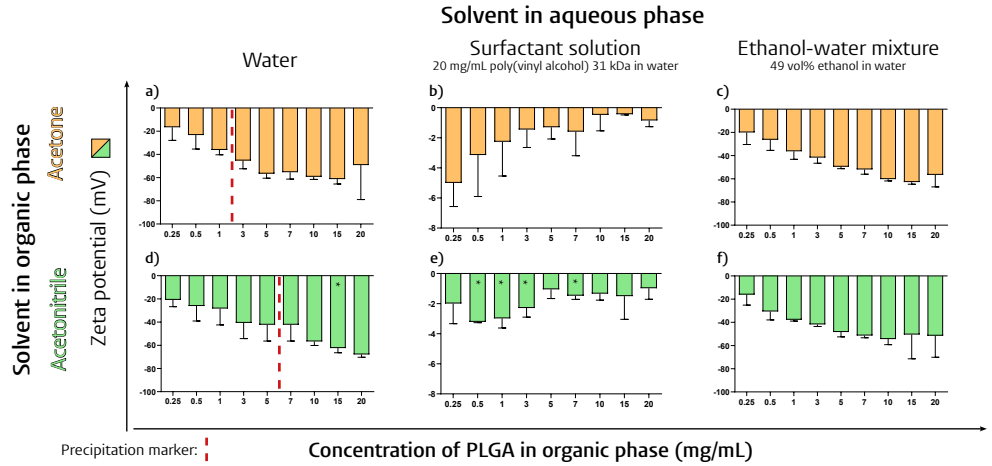

Figure 3. The influence of the PLGA concentration in the organic phase on the zeta potential of the formed PLGA nanoparticles, where the organic and aqueous phase consisted of a) acetone and ultrapure water, b) acetone and PVA in ultrapure water, c) acetone and an ethanol-water mixture d) acetonitrile and ultrapure water, e) acetonitrile and PVA in ultrapure water, f) and acetonitrile and an ethanol-water mixture, respectively. The TFR was 5,000 µL/min, and the FRR between the organic and the aqueous phase was 1:3. The precipitation marker indicates where the PLGA started to precipitate at the tip of the PEEK tube. Mean ± SD, n = 3 (*n = 2).

We compared the influence of the PLGA concentration on the formation of size-controlled nanoparticles in the microfluidic system for the different solvent combinations. The PLGA concentrations 0.25 and 0.5 mg/mL were excluded, as they had large standard deviations for some solvent combinations. A one-way analysis of variance with Tukey's multiple comparisons was performed to see if the PLGA particle diameters prepared with 1 mg/mL with different solvent combinations varied. The particles generated with the solvent combination "acetonitrile and PVA in ultrapure water" at a PLGA concentration of 1 mg/mL were significantly smaller than the ones generated with "acetone and ultrapure water" ($p = .022$) and "acetone and an ethanol-water mixture" ($p = .010$). To see if the particle formation followed different patterns after a PLGA concentration of 1 mg/mL, the slopes between the particle diameter and the PLGA concentration for the different solvent combinations were compared (Table 3).

The trend among the solvents was that the solvent combinations with acetone had lower slopes than the ones with acetonitrile, meaning that the particle diameter increases more with the increment of the PLGA concentration for the particles created with acetonitrile compared to the particles created with acetone. This was statistically corroborated by the slope of "acetone and ultrapure water" being statistically lower than its counterpart "acetonitrile and ultrapure water". The groups with PVA in ultrapure water (both with acetone and acetonitrile) had statistically higher slopes than the ones with ultrapure water and the ethanol-water mixture. This was shown by "acetone and PVA in ultrapure water" being significantly higher than the other groups with acetone and "acetonitrile and PVA in ultrapure water" being significantly higher than all the other groups, except for "acetone and PVA in ultrapure water". There was a trend of the groups with the ultrapure water having a slightly lower slope than the groups with the ethanol-water mixture.

Table 2. Pearson correlation coefficients showing the influence of the PLGA concentration on the particle diameter for the different solvent combinations and the influence of FRR or TFR on the particle diameter (see Table 1 for the combinations). A Pearson correlation coefficient shows the relationship between two variables; a value closer to +1 indicates a strong positive correlation, and a value closer to -1 indicates a strong inverse correlation. A two-tailed test measured the significance of the correlation coefficients. Not significant: $p > 0.05$, significant: $p < 0.05$. When performing the correlation statistics, the values for the flow rate ratios were set as the flow rate percentage from Syringe 2 (containing PLGA dissolved in organic solvent) out of the total flow, e.g., FRR 1:3 between Syringes 2 and 1 = 25%.

	Pearson correlation coefficient	P-value	Significant
Relationship between the PLGA concentration and the particle diameter for the solvents:			
Acetone and ultrapure water	0.64	$3.0 \cdot 10^{-4}$	Yes
Acetone and PVA in ultrapure water	0.91	$< 1.0 \cdot 10^{-10}$	Yes
Acetone and an ethanol-water mixture	0.92	$< 1.0 \cdot 10^{-10}$	Yes
Acetonitrile and ultrapure water	0.97	$< 1.0 \cdot 10^{-10}$	Yes
Acetonitrile and PVA in ultrapure water	0.97	$< 1.0 \cdot 10^{-10}$	Yes
Acetonitrile and an ethanol-water mixture	0.72	$2.6 \cdot 10^{-5}$	Yes
Relationship between the FRR or the TFR and particle diameter:			
FRR (percentage of the organic phase)	0.50	$5.9 \cdot 10^{-2}$	No
TFR	-0.85	$1.5 \cdot 10^{-7}$	Yes

The PLGA particle diameter is influenced by the TFR but not the FRR

Empty PLGA nanoparticles were prepared using the modular microfluidic system with different FRRs and TFRs. During the evaluation of the effect of FRR and TFR on the formation of nanoparticles, the PLGA concentration was maintained at 3 mg/mL, the organic solvent was acetonitrile, and the aqueous solvent was an ethanol-water mixture. Five FRRs (flow of the organic phase vs. flow of the aqueous phase) were tested (Table 1), while the TFR was kept constant (5 mL/min). When performing the correlation statistics, the values for the flow rate ratios were set as the flow rate percentage from Syringe 2 (containing the PLGA dissolved in the organic solvent) out of the total flow, e.g., FRR 1:3 between Syringes 2 and 1 = 25%. When testing the TFR, the FRR between the flow of the organic phase and the aqueous phase was kept constant (1:3). Eight TFRs were tested (see Table 1). The particle diameters and PDIs are summarised in Fig. 4a-b and the zeta potential data in Fig. 5a-b.

Table 3. Statistical comparisons of the formation of size-controlled nanoparticles via alteration of PLGA concentrations in the microfluidic system (linear regression curves) when using different solvents. The concentrations from 1 mg/mL to 20 mg/mL for the different solvent types were compared. Above the diagonal grey line: the p-values for the slope. Not significant: $p > 0.05$ (red), significant: $p < 0.05$ (green).

	Acetone and ultrapure water	Acetone and PVA in ultrapure water	Acetone and an ethanol-water mixture	Acetonitrile and ultrapure water	Acetonitrile and PVA in ultrapure water	Acetonitrile and an ethanol-water mixture
Equation	$y = 4.4 \cdot x + 77.4$	$y = 5.7 \cdot x + 77.4$	$y = 3.8 \cdot x + 84.0$	$y = 5.3 \cdot x + 61.4$	$y = 6.4 \cdot x + 54.2$	$y = 4.4 \cdot x + 64.1$
Acetone and ultrapure water		$3.9 \cdot 10^{-2}$	$1.9 \cdot 10^{-1}$	$4.6 \cdot 10^{-2}$	$1.2 \cdot 10^{-4}$	$9.7 \cdot 10^{-1}$
Acetone and PVA in ultrapure water			$5.8 \cdot 10^{-3}$	$5.2 \cdot 10^{-1}$	$3.4 \cdot 10^{-1}$	$5.1 \cdot 10^{-2}$
Acetone and an ethanol-water mixture				$4.2 \cdot 10^{-3}$	$1.3 \cdot 10^{-5}$	$2.7 \cdot 10^{-1}$
Acetonitrile and ultrapure water					$4.1 \cdot 10^{-2}$	$7.5 \cdot 10^{-2}$
Acetonitrile and PVA in ultrapure water						$5.1 \cdot 10^{-4}$
Acetonitrile and an ethanol-water mixture						

Correlation statistics were performed to see how the FRR or TFR affected the particle diameter (Table 2) (see Table S1 for the PDIs and zeta potentials). There was a significant inverse correlation between the TFR and the particle diameter, i.e., increasing the TFR led to smaller nanoparticles. In contrast, there was no correlation between the FRR (flow rate percentage of the organic phase) and the particle diameter. Both the PDI and zeta potential increased with a decrease in the organic phase flow rate percentage, and the zeta potentials increased at higher TFRs ($p < 0.05$). The PDI was not statistically significantly influenced by altering the TFR ($p > 0.05$).

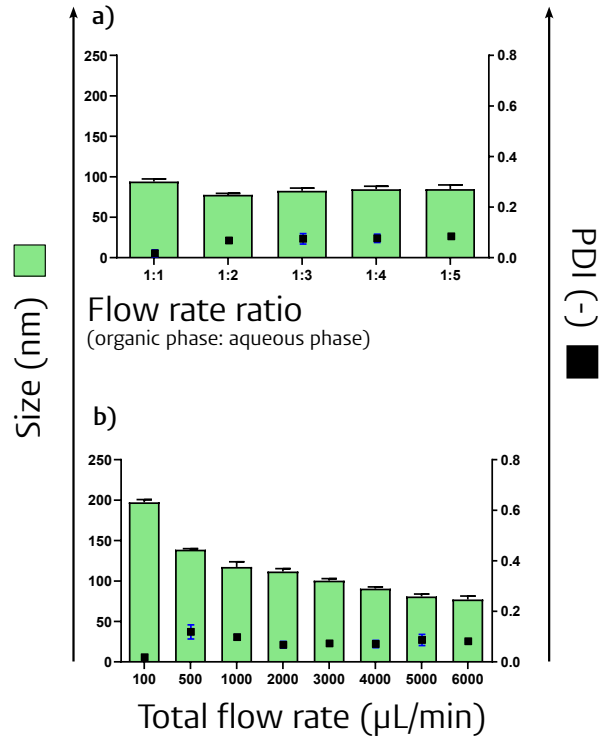

Figure 4. The influence of a) the FRR and b) the TFR on the nanoparticle diameter and PDI. The PLGA concentration was set to 3 mg/mL, the organic phase was acetonitrile, and the aqueous phase consisted of the ethanol-water mixture. The FRR between the organic and the aqueous phase for a) the TFR was 1:3, and the TFR for b) FRR was set to 5,000 µL/min. Mean ± SD, n = 3. PDI: polydispersity index.

The PLGA particle diameters increase with increasing amounts of lysozyme, while the diameter for ovalbumin-containing nanoparticles only changes slightly

Based on the results of the two-syringe system, a three-syringe system was designed to incorporate two water-soluble proteins with different physicochemical properties: i) ovalbumin, a 42.7 kDa protein [18] which is negatively charged at pH 7.4 [19], and ii) lysozyme, a 14.3 kDa protein [20], which is positively charged at pH 7.4 [21].

The particle diameters, PDIs, and encapsulation efficiencies of the proteins in the PLGA nanoparticles are reported in Fig. 6. For lysozyme, the particle diameter increases with the lysozyme-to-PLGA weight ratio until the particle diameter reaches 180 nm at a ratio of 1:16.7 ($p = .02$ between the ratio 1:50 and 1:16.7), whereafter, it reaches a plateau (Fig. 6a). The PDI is above 0.1 until the lysozyme-to-PLGA weight ratio reaches 1:16.7, whereafter it stays below 0.1 (PDI 1:12.5 compared to 1:100 $p = .006$, compared to 1:50 $p = .03$, compared to 1:25 $p = .0002$) (Fig. 6a). The encapsulation efficiency for lysozyme increases

until it reaches a lysozyme-to-PLGA weight ratio of 1:12.5 with an encapsulation efficiency of 85.2 ± 2.6%, whereafter it decreases to 67.4 ± 7.9% at the 1:10 weight ratio ($p = .01$ between 1:50 and 1:16.7, $p = .002$ between 1:25 and 1:12.5, and $p = .005$ between 1:12.5 and 1:10) (Fig. 6c). For ovalbumin, the particle diameter increases from the ovalbumin-to-PLGA weight ratio of 1:100 to 1:50, from 104.4 ± 1.0 nm to 112.8 ± 0.9 nm ($p = .02$), whereafter it decreases slightly from 101.2 ± 4.7 nm at 1:25 to 90.7 ± 1.6 nm at 1:10 ($p = .003$)((Fig. 6b). The PDI stays around 0.1 until an ovalbumin-to-PLGA weight ratio of 1:10 (Fig. 6b). The general trend is that the encapsulation efficiency for ovalbumin decreases with the increasing ovalbumin-to-PLGA weight ratio (Fig. 6d).

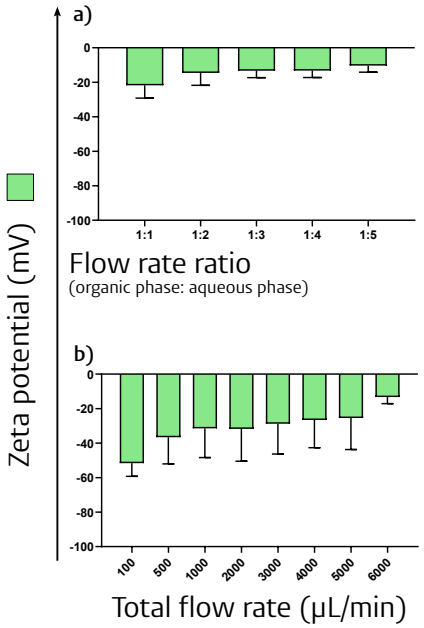

Figure 5. The influence of a)the FRR and b) the TFR on the zeta potential. The PLGA concentration was set to 3 mg/mL, the organic phase was acetonitrile, and the aqueous phase consisted of the ethanol-water mixture. The FRR between the organic and the aqueous phase for a) the TFR was 1:3, and the TFR for b) FRR was set to 5,000 µL/min. Mean ± SD, n = 3.

DISCUSSION

Traditional bulk processes for producing PLGA nanoparticles often have limitations as they are regularly associated with low throughput and lack of batch-to-batch consistency [11]. In comparison, microfluidics is a system of small channels, which allows for one-step assembly of the particles in a continuous manner [10, 12]. This leads to increased scalability, reduced production times, and precise control of the mixing, which makes it possible to tune the particle diameter [10, 12]. In summary, microfluidics have the potential to revolutionise drug delivery by offering more control over critical nanoparticulate formulation parameters.

In this study, we pursued three objectives: first, to set up a low-cost microfluidic system that does not rely on a microfluidic chip. Second, to investigate the parameters that affect the physicochemical properties of the PLGA nanoparticles using the microfluidic system. Lastly, to incorporate hydrophilic proteins into the PLGA nanoparticles.

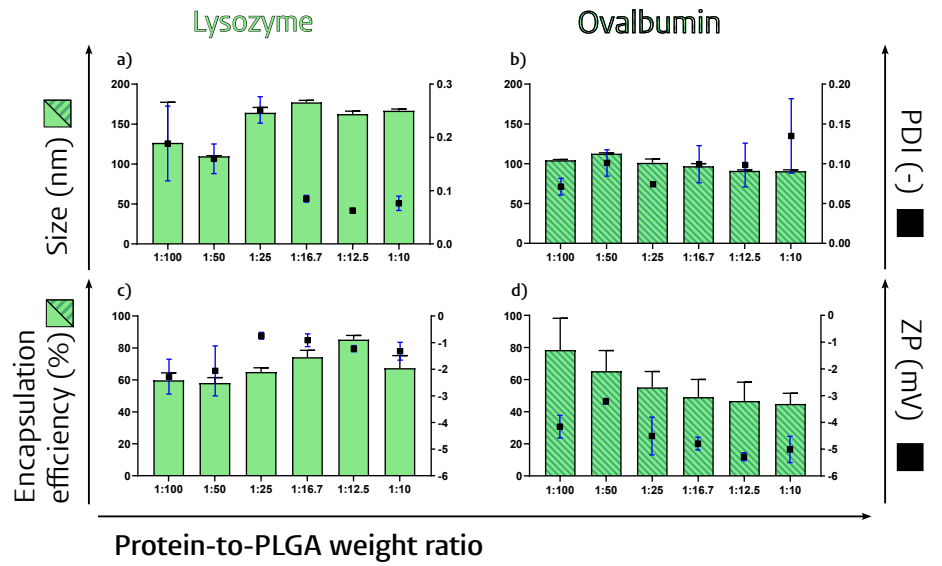

Figure 6. The influence of the protein-to-PLGA ratio for the protein lysozyme a) and ovalbumin b) on the size and PDI, and the encapsulation efficiency and zeta potential of lysozyme c) and ovalbumin d). Values represent mean ± SD, n = 3. ZP = zeta potential, PDI = polydispersity index.

We managed to set up a modular microfluidic system that produced nanoparticles with highly reproducible particle diameters, where an increasing particle diameter was obtained by increasing the PLGA concentration in the organic phase (increased the particle diameter from 33 to 180 nm) or by decreasing the TFR (increased particle diameters from 77 to 197 nm). In addition, the hydrophilic proteins ovalbumin and lysozyme were incorporated at different protein-to-PLGA weight ratios, resulting in encapsulation efficiencies above 40%.

Incorporation of proteins

The modular microfluidic system described in this paper can be adapted for multi-step processes. We decided to use a three-syringe setup for the incorporation of the proteins as we previously tested a two-syringe system versus a three-syringe system to prepare drug-loaded liposomes, where the three-syringe setup was advantageous (unpublished data). We chose

to incorporate the antigens ovalbumin and lysozyme into PLGA nanoparticles. Ovalbumin, a negatively charged protein at physiological pH, is readily available and is often used as a model antigen to study antigen-specific immune responses in mice [22]. In opting for a protein possessing distinct attributes from ovalbumin, we selected lysozyme for its low cost and positive charge at physiological pH [20, 21]. The aqueous solvent PVA in ultrapure water was chosen for both proteins as the proteins aggregated visibly with higher concentrations of ovalbumin, when the solvent combination of the ethanol-water mixture was used, and because PLGA precipitated at higher concentrations, when ultrapure water was used.

The PLGA concentration for creating the PLGA nanoparticles with incorporated proteins was set to 3 mg/mL for lysozyme and 5 mg/mL for ovalbumin. These concentrations were chosen to create particles of around 100 nm. While the particle diameter stayed around 100 nm for ovalbumin, it increased with the lysozyme-to-PLGA weight ratio from 110 nm (1:100) to 177 nm (1:16.7), whereafter it dropped slightly. This is likely due to the positive charge of lysozyme that attracts the negatively charged PLGA. We measured the encapsulation efficiencies of ovalbumin and lysozyme. Ovalbumin had an encapsulation efficiency of 44–78% where the encapsulation efficiency decreased with increasing amounts of ovalbumin. The encapsulation efficiency for lysozyme was 58–85%, where the highest encapsulation efficiency was at the lysozyme-to-PLGA weight ratio of 1:12.5. While our focus remained on a lactide:glycolide 50:50 polymer, other investigations have explored the impact of various PLGA polymers on encapsulation efficiency and particle diameter. They found that lactide:glycolide 85:15 polymer demonstrated higher encapsulation efficiency of ovalbumin [17], this aspect could be a worthwhile avenue for future exploration.

The modular microfluidic system used in this study has also been used to prepare PLGA particles for opalescence studies [23] and to incorporate the lipid dye (2*Z*)-2-[(*E*)-3-(3,3-dimethyl-1-octadecylindol-1-ium-2-yl)prop-2-enylidene]-3,3-dimethyl-1-octadecylindole; perchlorate into PLGA particles of various sizes with the two-syringe system, where the lipid was dissolved in the organic phase, to visualise the uptake of PLGA particles of different sizes in zebrafish [24]. Furthermore, ovalbumin and oligonucleotide 1826 (a Class B CpG oligonucleotide; a murine TLR9 ligand) into PLGA nanoparticles for incorporation into dissolving nanoparticles [25]. If another lipophilic substance should be incorporated into the PLGA nanoparticles, it could be dissolved in the organic solvent together with the PLGA. If a compound that is not dissolvable in the organic phase or water should be incorporated, it could possibly be dissolved in another solvent and be incorporated with the three-syringe system. The modular microfluidic system has also been used to prepare polymer-lipid hybrids, which are particles with a PLGA core surrounded by a lipid layer(s) (submitted manuscript by Mikolaj Szachniewicz et al.), by adding an extra attachment to the system, making it a four-syringe system.

The choice of the microfluidic settings

The chosen materials (polymers, drugs, surfactants) and settings (flow rates, channel geometries) used in microfluidic systems affect the physicochemical characteristics of the formed empty PLGA particles. Therefore, we tested how PLGA concentrations, solvents, FRR, and TFR affected the particle formation in this system. The nanoparticle diameters in our study ranged from 32 to 197 nm. The sizes are normally larger with conventional methods, as double-emulsion and nanoprecipitation methods lead to PLGA nanoparticles with a minimum particle diameter of around 150 nm [7, 26]. According to some existing literature, FRR influences the PLGA particle diameter where an increase in the rate of the aqueous solvent correlates with a reduction in particle diameter [17, 27]. However, this is not always the case, as the FRR did not affect the particle diameter in another study [28]. The FRR did not significantly affect the particle diameter in our system; however, there was a trend towards smaller particles with an increased rate of the aqueous solvent (i.e., decreased rate of organic solvent). An increase in TFR correlated with a reduction in PLGA particle diameter, similar to the literature [17, 28].

Our study revealed that the choice of solvent affects the PLGA particle diameter. We tested two organic solvents and three aqueous solvents in our microfluidic system. The particle diameter increased with an increasing PLGA concentration in the organic solvent for all the solvent combinations.

The organic solvents acetone and acetonitrile were chosen as they are both miscible with water [29] because we were aiming for nanoprecipitation microfluidics, also called continuous microfluidics, which tend to generate nano-sized particles [13]. The organic solvent acetone generated larger particle diameters than acetonitrile (at a PLGA concentration of 1 mg/mL), which is also shown in another microfluidic setup [30]. This is likely due to the diffusion coefficient of acetonitrile in water being higher than the diffusion coefficient of acetone in water which favours the formation of smaller nanoparticles [31]. However, we observed that the size difference was reduced when the PLGA concentration was increased. Adding PVA to ultrapure water generated smaller nanoparticles than the ethanol-water mixture and ultrapure water at low PLGA concentrations. However, smaller particle diameters at low concentrations could be due to the formation of PVA micelles, as acetonitrile without PLGA with 20 mg/mL PVA in ultrapure water led to particle diameters of 19.7 ± 8.7 nm. The knowledge of how the solvent affects the particle diameter can be used to generate nanoparticles with a specific particle diameter, e.g., if the goal is to prepare small nanoparticles, the combination of a low concentration of PLGA in acetonitrile together with PVA in ultrapure water could be used.

Using ultrapure water as the aqueous phase led to PLGA precipitation on the PEEK tube at concentrations higher than 1 mg/mL PLGA in acetone and 5 mg/mL in acetonitrile. This is probably due to the lack of PLGA particle stabilisation in ultrapure water, whereas PVA can stabilise the particle formation [32]. The nanoparticle formulations prepared with PVA

in ultrapure water had neutral zeta potentials (-5 to 0 mV). In comparison, nanoparticles prepared with ultrapure water or the ethanol-water mixture had negative zeta potentials (-16 to -68 mV). This is likely due to the PVA layer on the surface of the NPs that shields the charge [33]. The different aqueous solvents have pros and cons. By using the ultrapure water, no ethanol or excess PVA is added, which, depending on the application, possibly would need to be removed. However, using ultrapure water did not stabilise the particles over a certain PLGA concentration. This led to a lower PLGA concentration in the produced formulation, as the PLGA precipitated in the PEEK tube. The PVA stabilises the particle formation but leads to a neutral charge and a possible surplus of surfactant in the formulation. However, this can be advantageous as PVA can stabilise the PLGA particles during freeze-drying [34]. The PVA concentration can be adjusted to determine the optimal concentration to stabilise the particles while creating a minimal PVA surplus in the formulation. The ethanol-water mixture leads to a negative charge while creating a surplus of ethanol that, dependent on the application, needs to be removed. However, it seems to stabilise the production of empty PLGA particles.

The modular microfluidic system: technical aspects

Initially, a microfluidic setup with two syringes was established. The components within the microfluidic system were thoughtfully selected to ensure cost-effectiveness. The pumps were low-cost (NE300 (single) syringe pumps (ProSense B.V.)) while it still was possible to adjust the speed by using syringes with different IDs. Syringes with a larger ID were able to generate higher flow rates as the turning screw that pushed on the syringe plunger flange had a maximum speed. Therefore, 10 mL syringes were used to contain the aqueous and organic phases to ensure a high flow rate while still being able to fit within the clamp. A 500-µL syringe was used to contain the aqueous proteins as i) it was possible to see the piston move when starting the pump (to ensure that the block pushing on the piston was installed correctly). And ii) because it would lead to less solvent loss, thereby ensuring less protein loss, as there was a dead volume in the plain tip, and also because the pump needed to be stopped before the plunger hit the plain tip, the end of the syringe, to not damage it.

For our microfluidics system, we selected components with excellent chemical stability against the used solvents at room temperature. The fluid path of the syringes consisted of a PTFE-tipped plunger and a borosilicate glass syringe with PTFE Luer-lock terminations [35–37], which are made of highly chemically inert materials [38, 39]. Gastight® syringes are leak-free, ensuring a flow without the risk of air intake [37]. The PEEK tube, the CapTite™ Luer-lock adapters, fittings, and adapters were made of PEEK, which is commonly used in chromatography and is also an inert material [40]. PTFE and PEEK are resistant to acetone, acetonitrile, ethyl acetate, water, and ethanol [41]. The interconnect tees were crafted from polyetherimide, which has good chemical resistance; however, it is not recommended for use with acetone and ethyl acetate at elevated temperatures (>50°C) [42, 43]. Despite the chemical resistance of the selected microfluidic-system components, we carefully inspected the different components before and after each nanoparticle preparation run. We did not notice damage on the interconnect tee's screwing mechanism after the use of acetone, however, it did lead to a slightly shiny surface after extended immersion in acetone. If an interconnect tee in PEEK or PTFE could be found that would be preferable.

Polyimide-coated fused silica capillary tubing with IDs of 75 µm and 250 µm and ODs of approximately 360 µm had polyimide coatings of 20 µm and 18 µm, respectively [44]. This meant that the capillary with an ID of 250 µm had a silica layer of approximately 30 µm, while the capillary with an ID of 75 µm had a silica layer of approximately 110 µm. While the capillary with an ID of 75 µm kept its integrity for days, the capillary with an ID of 250 µm tended to break after a few minutes due to its thin silica layer. Unfortunately, it was not possible to use a capillary with an ID of 75 µm for the syringe containing the organic phase, as the syringe pump could not generate the required amount of force required for the high flow rate on the syringe plunger without the drive-screw malfunctioning. Therefore, it is advisable to pre-test capillaries with large IDs to determine the retainment of their integrity at high flow rates/pressures.

CONCLUSION

We successfully developed a modular microfluidic system based on easily cleanable block components, ensuring minimal clogging and on-the-spot modifications. Through our investigations, we identified critical process parameters in the production that could affect the physicochemical properties of the PLGA nanoparticles.

The formation of the nanoparticles was affected by the PLGA concentration in the organic solvent and the total flow rate. The solvent in the aqueous phase affected the stability of the PLGA nanoparticles and the zeta potential. We effectively achieved the incorporation of the biomacromolecules ovalbumin and lysozyme with encapsulation efficiencies above 40%, showing the potential to formulate subunit vaccines and therapeutic proteins for controlled release utilising this method. Altogether, our system is a low-cost and highly versatile modular microfluidic platform that can produce PLGA nanoparticles in a highly reproducible manner with and without encapsulated protein.

References

1. Rao JP, Geckeler KE. Polymer nanoparticles: Preparation techniques and size-control parameters. Prog Polym Sci. 2011;36(7):887-913. https://doi.org/10.1016/j.progpolymsci.2011.01.001.
2. Danhier F, Ansorena E, Silva JM, Coco R, Le Breton A, Préat V. PLGA-based nanoparticles: an overview of biomedical applications. J Control Release. 2012;161(2):505-22. https://doi.org/10.1016/j.jconrel.2012.01.043.
3. Prabhu P, Patravale V. Potential of nanocarriers in antigen delivery: the path to successful vaccine delivery. Nanocarriers. 2014;1:10-45. https://doi.org/10.2478/nanca-2014-0001.
4. Zhang Y, García-Gabilondo M, Grayston A, Feiner IVJ, Anton-Sales I, Loiola RA, et al. PLGA protein nanocarriers with tailor-made fluorescence/MRI/PET imaging modalities. Nanoscale. 2020;12(8):4988-5002. https://doi.org/10.1039/C9NR10620K.
5. Acharya S, Sahoo SK. PLGA nanoparticles containing various anticancer agents and tumour delivery by EPR effect. Adv Drug Deliv Rev. 2011;63(3):170-83. https://doi.org/10.1016/j.addr.2010.10.00.
6. Varypataki EM, Silva AL, Barnier-Quer C, Collin N, Ossendorp F, Jiskoot W. Synthetic long peptide-based vaccine formulations for induction of cell mediated immunity: A comparative study of cationic liposomes and PLGA nanoparticles. J Control Release. 2016;226:98-106. https://doi.org/10.1016/j.jconrel.2016.02.018.
7. Mönkäre J, Pontier M, van Kampen EEM, Du G, Leone M, Romeijn S, et al. Development of PLGA nanoparticle loaded dissolving microneedles and comparison with hollow microneedles in intradermal vaccine delivery. Eur J Pharm Biopharm. 2018;129:111-21. https://doi.org/10.1016/j.ejpb.2018.05.031.
8. Ghitman J, Biru EI, Stan R, Iovu H. Review of hybrid PLGA nanoparticles: Future of smart drug delivery and theranostics medicine. Mater Des. 2020;193:108805. https://doi.org/10.1016/j.matdes.2020.108805.
9. Operti MC, Bernhardt A, Grimm S, Engel A, Figdor CG, Tagit O. PLGA-based nanomedicines manufacturing: Technologies overview and challenges in industrial scale-up. Int J Pharm. 2021;605:120807. https://doi.org/10.1016/j.ijpharm.2021.120807.
10. Astete CE, Sabliov CM. Synthesis and characterization of PLGA nanoparticles. J Biomater Sci Polym Ed. 2006;17(3):247-89. https://doi.org/10.1163/156856206775997322.
11. Streck S, Neumann H, Nielsen HM, Rades T, McDowell A. Comparison of bulk and microfluidics methods for the formulation of poly-lactic-co-glycolic acid (PLGA) nanoparticles modified with cell-penetrating peptides of different architectures. Int J Pharm X. 2019;1:100030. https://doi.org/10.1016/j.ijpx.2019.100030.
12. Valencia PM, Farokhzad OC, Karnik R, Langer R. Microfluidic technologies for accelerating the clinical translation of nanoparticles. Nat Nanotechnol. 2012;7(10):623-9. https://doi.org/10.1038/nnano.2012.168.
13. Rezvantalab S, Keshavarz Moraveji M. Microfluidic assisted synthesis of PLGA drug delivery systems. RSC Adv. 2019;9(4):2055-72. https://doi.org/10.1039/c8ra08972h.
14. Benne N, van Duijn J, Kuiper J, Jiskoot W, Slütter B. Orchestrating immune responses: How size, shape and rigidity affect the immunogenicity of particulate vaccines. J Control Release. 2016;234:124-34. https://doi.org/10.1016/j.jconrel.2016.05.033.
15. Silva AL, Soema PC, Slütter B, Ossendorp F, Jiskoot W. PLGA particulate delivery systems for subunit vaccines: Linking particle properties to immunogenicity. Hum Vaccin Immunother. 2016;12(4):1056-69. https://doi.org/10.1080/21645515.2015.1117714.
16. Albanese A, Tang PS, Chan WC. The effect of nanoparticle size, shape, and surface chemistry on biological systems. Annu Rev Biomed Eng. 2012;14:1-16. https://doi.org/10.1146/annurev-bioeng-071811-150124.
17. Roces CB, Christensen D, Perrie Y. Translating the fabrication of protein-loaded poly(lactic-co-glycolic acid) nanoparticles from bench to scale-independent production using microfluidics. Drug Deliv Transl Res. 2020;10(3):582-93. https://doi.org/10.1007/s13346-019-00699-y.
18. Nisbet AD, Saundry RH, Moir AJ, Fothergill LA, Fothergill JE. The complete amino-acid sequence of hen ovalbumin. Eur J Biochem. 1981;115(2):335-45. https://doi.org/10.1111/j.1432-1033.1981.tb05243.x.
19. van der Maaden K, Yu H, Sliedregt K, Zwier R, Leboux R, Oguri M, et al. Nanolayered chemical modification of silicon surfaces with ionizable surface groups for pH-triggered protein adsorption and release: application to microneedles. J Mater Chem B. 2013;1(35):4466-77. https://doi.org/10.1039/c3tb20786b.
20. Canfield RE. The Amino Acid Sequence of Egg White Lysozyme. J Biol Chem. 1963;238(8):2698-707. https://doi.org/10.1016/S0021-9258(18)67888-3.
21. Wetter L, Deutsch H. Immunological studies on egg white proteins: IV. Immunochemical and physical studies of lysozyme. J Biol Chem. 1951;192(1):237-42. https://doi.org/10.1016/S0021-9258(18)55926-3.
22. Taconic Biosciences. Immunology: Ovalbumin (OVA) Challenge [Internet]. https://www.taconic.com/find-your-model/gems/cryopreserved-models/knockout-repository/phenotypic-data-packages/comprehensive/ovalbumin-challenge.html. Accessed 04 Mar 2024.
23. Kunz P, Stuckenberger E, Hausmann K, Gentiluomo L, Neustrup M, Michalakis S, et al. Understanding opalescence measurements of biologics - A comparison study of methods, standards, and molecules. Int J Pharm. 2022;628:122321. https://doi.org/10.1016/j.ijpharm.2022.122321.
24. Arias-Alpizar G, Koch B, Hamelmann NM, Neustrup MA, Paulusse JMJ, Jiskoot W, et al. Stabilin-1 is required for the endothelial clearance of small anionic nanoparticles. Nanomedicine : nanotechnology, biology, and medicine. 2021;34:102395. https://doi.org/10.1016/j.nano.2021.102395.
25. Lee J, Neustrup MA, Slütter B, O'Mahony C, Bouwstra JA, van der Maaden K. Intradermal Vaccination with PLGA Nanoparticles via Dissolving Microneedles and Classical Injection Needles. Pharm Res. 2024;41(2):305-19. https://doi.org/10.1007/s11095-024-03665-7.
26. Hajavi J, Ebrahimian M, Sankian M, Khakzad MR, Hashemi M. Optimization of PLGA formulation containing protein or peptide-based antigen: Recent advances. J Biomed Mater Res A. 2018;106(9):2540-51. https://doi.org/10.1002/jbm.a.36423.
27. Karnik R, Gu F, Basto P, Cannizzaro C, Dean L, Kyei-Manu W, et al. Microfluidic Platform for Controlled Synthesis of Polymeric Nanoparticles. Nano Lett. 2008;8(9):2906-12. https://doi.org/10.1021/nl801736q.
28. Bao Y, Maeki M, Ishida A, Tani H, Tokeshi M. Preparation of size-tunable sub-200 nm PLGA-based nanoparticles with a wide size range using a microfluidic platform. PLoS One. 2022;17(8):e0271050. https://doi.org/10.1371/journal.pone.0271050.
29. Merck. Solvent Miscibility Table [Internet]. https://www.sigmaaldrich.com/NL/en/technical-documents/technical-article/analytical-chemistry/purification/solvent-miscibility-table. Accessed 18 Sep 2024.
30. Lababidi N, Sigal V, Koenneke A, Schwarzkopf K, Manz A, Schneider M. Microfluidics as tool to prepare size-tunable PLGA nanoparticles with high curcumin encapsulation for efficient mucus penetration. Beilstein J Nanotechnol. 2019;10:2280-93. https://doi.org/10.3762/bjnano.10.220.
31. Huang W, Zhang C. Tuning the Size of Poly(lactic-co-glycolic Acid) (PLGA) Nanoparticles Fabricated by Nanoprecipitation. Biotechnol J. 2018;13(1). https://doi.org/10.1002/biot.201700203.
32. Stromberg ZR, Lisa Phipps M, Magurudeniya HD, Pedersen CA, Rajale T, Sheehan CJ, et al. Formulation of stabilizer-free, nontoxic PLGA and elastin-PLGA nanoparticle delivery systems. Int J Pharm. 2021;597:120340. https://doi.org/10.1016/j.ijpharm.2021.120340.
33. Sahoo SK, Panyam J, Prabha S, Labhasetwar V. Residual polyvinyl alcohol associated with poly (D,L-lactide-co-glycolide) nanoparticles affects their physical properties and cellular uptake. J Control Release. 2002;82(1):105-14. https://doi.org/10.1016/s0168-3659(02)00127-x.
34. Andreana I, Bincoletto V, Manzoli M, Rodà F, Giarraputo V, Milla P, et al. Freeze Drying of Polymer Nanoparticles and Liposomes Exploiting Different Saccharide-Based Approaches. Materials (Basel). 2023;16(3). https://doi.org/10.3390/ma16031212.
35. Fischer Scientific. Hamilton™ 1000 Series Gastight™ Syringes: Luer Lock Syringes, TLL Termination [Internet]. https://www.fishersci.nl/shop/products/hamilton-1000-series-gastight-syringes-luer-lock-syringes-tll-termination-14/10374902. Accessed 25 Mar 2024.
36. Hamilton Company. 500 µL Gastight Syringe Model 1750 TLL, PTFE Luer Lock, Needle Sold Separately [Internet]. https://www.hamiltoncompany.com/laboratory-products/syringes/81220. Accessed 25 Mar 2024.
37. Hamilton Company. Hamilton Reference Guide SYRINGES & NEEDLES 2023. Lit. No. L20097 Rev. D — 09/2023. https://assets-labs.

hamiltoncompany.com/File-Uploads/Syringe_Needle_Reference-Guide.pdf?v=1696888429.
38. Nag A, Baksi A, Ghosh J, Kumar V, Bag S, Mondal B, et al. Tribochemical Degradation of Polytetrafluoroethylene in Water and Generation of Nanoplastics. ACS Sustain Chem Eng. 2019;7(21):17554-8. https://doi.org/10.1021/acssuschemeng.9b03573.
39. CP Lab Safety. PTFE and Teflon Chemical Compatibility [Internet]. https://www.calpaclab.com/teflon-ptfe-compatibility/. Accessed 26 Mar 2024.
40. CP Lab Safety. PEEK Chemical Compatibility [Internet]. https://www.calpaclab.com/polyetherether-ketone-peek-chemical-compatibility-chart/. Accessed 26 Mar 2024.
41. VICI AG International. Chromatography Fluid/Gas Transfer 2009. Catalog 10 Int. p. 108-9. https://www.greyhoundchrom.com/Content/Images/uploaded/files/Vici%20Jour/Vici%20Jour.pdf.
42. Advanced Sensor Technologies I. ULTEM - PEI (Poly-Ether-Imide) Chemical Resistance Chart. https://www.astisensor.com/ultem.pdf.
43. Thermo Fischer Scientific. Labware Chemical Resistance Table. https://tools.thermofisher.com/content/sfs/brochures/D20480.pdf.
44. BGB. TSP - Standard Polyimide Coating [Internet]. https://www.bgb-info.com/home.php?cat=303. Accessed 26 Mar 2024.

SUPPLEMENTARY MATERIAL

Table S1. Pearson correlation coefficient showing the influence of the PLGA concentration on the PDI or zeta potential for the different solvent combinations, FRR or TFR (see Table 1 for the combinations). The Pearson correlation coefficient shows the relationship between two variables, a value closer to +1 indicates a strong positive correlation, and a value closer to -1 indicates a strong inverse correlation. The significance of the correlation coefficients was measured by a two-tailed test. Not significant: $p > .05$, significant: $p < .05$. When performing the correlation statistics, the values for the flow rate ratios were set as the flow rate percentage from Syringe 2 (containing PLGA dissolved in organic solvent) out of the total flow, e.g., FRR 1:3 between Syringes 2 and 1 = 25%.

	Pearson correlation coefficient	p-value	Significant
PDI			
Acetone and ultrapure water	-0.46	$1.5 \cdot 10^{-2}$	Yes
Acetone and PVA in ultrapure water	-0.65	$2.4 \cdot 10^{-4}$	Yes
Acetone and an ethanol-water mixture	-0.31	$1.1 \cdot 10^{-1}$	No
Acetonitrile and ultrapure water	-0.54	$3.4 \cdot 10^{-3}$	Yes
Acetonitrile and PVA in ultrapure water	-0.70	$4.3 \cdot 10^{-5}$	Yes
Acetonitrile and an ethanol-water mixture	-0.50	$6.9 \cdot 10^{-3}$	Yes
FRR	-0.87	$2.2 \cdot 10^{-5}$	Yes
TFR	0.12	$5.6 \cdot 10^{-1}$	No
Zeta potential			
Acetone and ultrapure water	-0.55	$2.8 \cdot 10^{-3}$	Yes
Acetone and PVA in ultrapure water	0.53	$4.7 \cdot 10^{-3}$	Yes
Acetone and an ethanol-water mixture	-0.77	$3.2 \cdot 10^{-6}$	Yes
Acetonitrile and ultrapure water	-0.83	$1.7 \cdot 10^{-7}$	Yes
Acetonitrile and PVA in ultrapure water	0.50	$1.5 \cdot 10^{-2}$	Yes
Acetonitrile and an ethanol-water mixture	-0.58	$1.7 \cdot 10^{-3}$	Yes
FRR	-0.63	$1.3 \cdot 10^{-2}$	Yes
TFR	0.56	$4.9 \cdot 10^{-3}$	Yes